NASA TECHNICAL MEMORANDUM

NASA TM X-2194

NASA TM X-2194

OVERALL PERFORMANCE IN ARGON OF A 3.7-INCH SIX-STAGE AXIAL-FLOW COMPRESSOR

by Edward R. Tysl, Laurence J. Heidelberg, and Carl Weigel

Lewis Research Center
Cleveland, Ohio 44135

NATIONAL AERONAUTICS AND SPACE ADMINISTRATION • WASHINGTON, D. C. • MARCH 1971

1. Report No.	2. Government Accession No.	3. Recipient's Catalog No.
NASA TM X-2194		

4. Title and Subtitle	5. Report Date
OVERALL PERFORMANCE IN ARGON OF A 3.7-INCH SIX-STAGE AXIAL-FLOW COMPRESSOR	March 1971
	6. Performing Organization Code

7. Author(s)	8. Performing Organization Report No.
Edward R. Tysl, Laurence J. Heidelberg, and Carl Weigel	E-5522
	10. Work Unit No. 120-27

9. Performing Organization Name and Address	11. Contract or Grant No.
Lewis Research Center National Aeronautics and Space Administration Cleveland, Ohio 44135	
	13. Type of Report and Period Covered
12. Sponsoring Agency Name and Address	Technical Memorandum
National Aeronautics and Space Administration Washington, D.C. 20546	14. Sponsoring Agency Code

15. Supplementary Notes

16. Abstract

Overall performance from the compressor inlet to the collector exit and overall performance from the compressor inlet to the exit of the sixth-stage stator is presented as a function of equivalent weight flow. Peak efficiency (compressor inlet to collector exit) was 0.755 at the design equivalent rotative speed of 49 213 rpm and occurred at an equivalent weight flow of 1.55 lb/sec (0.70 kg/sec). The pressure ratio at peak efficiency was 2.72.

17. Key Words (Suggested by Author(s))	18. Distribution Statement
Axial-flow compressor Overall performance Space power Brayton cycle	Unclassified - unlimited

19. Security Classif. (of this report)	20. Security Classif. (of this page)	21. No. of Pages	22. Price*
Unclassified	Unclassified	22	$3.00

*For sale by the National Technical Information Service, Springfield, Virginia 22151

Page Intentionally Left Blank

OVERALL PERFORMANCE IN ARGON OF A 3.7-INCH SIX-STAGE AXIAL-FLOW COMPRESSOR

by Edward R. Tysl, Laurence J. Heidelberg, and Carl Weigel

Lewis Research Center

SUMMARY

A 3.7-inch (9.4-cm) diameter six-stage axial-flow compressor applicable for a 10-kilowatt Brayton cycle space electrical power generation system was tested in argon at an inlet pressure of 6 psia (41×10^3 N/m^2 abs). Overall performance from the compressor inlet to the collector exit and overall performance from the compressor inlet to the exit of the sixth-stage stator is presented as a function of equivalent weight flow. Peak efficiency (compressor inlet to collector exit) was 0.755 at the design equivalent rotative speed of 49 213 rpm and occurred at an equivalent weight flow of 1.55 pounds per second (0.70 kg/sec). The pressure ratio at peak efficiency was 2.72. The design values of efficiency, weight flow, and pressure ratio were 0.825, 1.52 pounds per second (0.69 kg/sec), and 2.30, respectively. It is reasoned that the higher than design pressure ratio may be a result of the actual deviation angles and or flow boundary layer blockages being lower than that assumed in the design. The design values of deviation angles were increased above normal design practice to compensate for an expected Reynolds number effect on this parameter which may not have materialized. Lower than design efficiency may in part be a result of the mismatching of flow angles within the machine due to the higher than design pressure ratio.

INTRODUCTION

Interest in generating electric power in space resulted in a series of studies (refs. 1 to 4) concerning cycle selection and cycle components. For small power systems, the Brayton cycle was found to have good potential. The studies indicated that turbomachinery component efficiencies were one of the prime factors in establishing overall system weight. In order to establish the attainable efficiency levels of compressor components suitable in size for a 10-kilowatt Brayton cycle power system, a compressor

research program was initiated at the NASA Lewis Research Center. This program included investigating both a radial bladed centrifugal compressor (refs. 5 and 6) and an axial-flow compressor.

The axial-flow compressor design and fabrication (ref. 7) was accomplished on contract with Pratt & Whitney Aircraft, Division of United Aircraft Corporation, East Hartford, Connecticut. Preliminary testing for mechanical integrity was conducted at the contractor's plant. The overall compressor performance presented herein was obtained at the Lewis Research Center.

Overall argon performance is presented for six speeds from 50 to 100 percent of design speed. Data were obtained over a range of weight flows at each speed from maximum flow to stall conditions. The data were taken with the compressor inlet pressure set at 6 psia (41×10^3 N/m^2 abs), the design value. Performance is presented based on the flow conditions at the compressor inlet and stator 6 exit and the flow condition at the compressor inlet and collector exit.

SYMBOLS

IGV	inlet guide vanes
N	compressor rotational speed, rpm
$N/\sqrt{\theta}$	equivalent rotative speed, rpm
P	total (stagnation) pressure, psia; N/m^2 abs
p	static pressure, psia; N/m^2 abs
$R_1, \ldots, R_6$	inlet to rotor blade row 1, . . ., rotor blade row 6
$S_1, \ldots, S_6$	inlet to stator blade row 1, . . ., stator blade row 6
T	total (stagnation) temperature, $^{\circ}$R; K
U	blade speed, ft/sec; m/sec
$\frac{U}{\sqrt{\theta}}$	equivalent blade speed, ft/sec; m/sec
W	weight (mass) flow, lb/sec; kg/sec
$\frac{W\sqrt{\theta}}{\delta}$	equivalent weight (mass) flow, lb/sec; kg/sec
γ	ratio of specific heat at constant pressure to specific heat at constant volume for argon, 1.667
δ	ratio of compressor inlet total pressure to NASA standard sea level pressure, P_0/14.7 psia; $P_0/101\times10^3$ N/m^2 abs

η_{0-7} adiabatic efficiency - station 0 to station 7, $T_0\left[(P_7/P_0)^{(\gamma-1)/\gamma} - 1\right]\Big/(T_7 - T_0)$

η_{0-8} adiabatic efficiency - station 0 to station 8, $T_0\left[(P_8/P_0)^{(\gamma-1)/\gamma} - 1\right]\Big/(T_7 - T_0)$

θ ratio of compressor inlet total temperature to NASA sea level temperature, $T_0/518.7^{\circ}$ R; $T_0/288.2$ K

Subscripts:

t rotor tip

0 station in inlet pipe ($\cong$ 10 in. or 25.4 cm upstream of compressor inlet flange)

7 station at stator 6 exit, diffuser inlet

8 station in exit pipe (2.5 in. or 6.4 cm downstream of collector exit flange)

COMPRESSOR DESIGN

A detailed description of the aerodynamic and mechanical design and of the analysis made in arriving at the design values is given in reference 7. A summary of the design is presented herein.

The values of the overall compressor design parameters are presented in table I. Also included in table I are the equivalent design values for standard inlet conditions. The compressor was designed having six stages. It incorporated inlet guide vanes which were designed to impart a swirl in the direction of rotation of 15° from the axial direction at the vane tip. This swirl was reduced linearly to zero at the hub. The swirl level and distribution was maintained at the exit of each stator except for stator 6 which turns the flow to the axial direction at all radii. The design tip speed is 811.6 feet per second (246.5 m/sec) for rotor 1 inlet. The corresponding inlet relative Mach number is 0.788. The hub-tip radius ratio at rotor 1 inlet is 0.69 and increases to 0.73 at stator 6 exit. The hub diameter was held constant through the machine. The through flow velocity at midpassage was decreased from 404 feet per second (123 m/sec) at rotor 1 inlet to 305 feet per second (93 m/sec) at stator 6 exit. Rotor tip diffusion factors varied from 0.42 for rotor 1 to 0.37 for rotor 6. The stator hub diffusion factors varied from 0.44 for stator 1 to 0.39 for stator 4. The stator hub loading then increased to 0.45 for stator 6.

The following design values for each blade row of this compressor are tabulated in reference 7: thermodynamic conditions, gas velocities, actual and effective flow areas, blade loading parameters, Reynolds numbers, incidence angles, deviation angles, and blade geometry parameters.

In arriving at the final compressor design, deviation angles were increased above

values arrived at by normal design rules based on the data presented in reference 8. The data presented in this reference showed that an increase in deviation angles could be expected at the low Reynolds numbers (maximum blade chord Reynolds number of 106 300 at the tip element of rotor 1 to a minimum Reynolds number of 52 200 at the hub element of stator 6) at which the blading must operate. The design deviation angles presented in reference 7 include the increase due to the expected Reynolds number effect.

APPARATUS AND PROCEDURE

Test Apparatus

A photograph of the assembled six-stage rotor and surrounding inner casing is presented in figure 1. The rotor is a bolted assembly consisting of three components, front shaft, rotor drum, and rear shaft. The rotor blades were machined from a titanium alloy (AMS 4928) and are attached to the rotor drum by dovetails and secured by pins. The stator vanes were made of stainless steel and were brazed into semicircular assemblies consisting of an inner and outer shroud ring. The inner shroud ring of the stator vane assemblies had labyrinth seals which minimized recirculation of argon gas flow from stator discharge back to the stator inlet. The stator inner seal clearances and rotor blade tip clearances were 0.006 and 0.007 inch (0.015 and 0.018 cm), respectively. In order to prevent possible blade tip damage during compressor operation an abradable material was placed in the housing over the rotor blade tips.

Figure 2 presents a cross-sectional drawing of the compressor research package. The rotor is supported by two spring mounted, axially loaded oil lubricated ball bearings. The two bearing compartments are sealed from the argon compressor working fluid by two carbon face seals. Scavenge pressure in the bearing compartments was maintained at a level below argon gas pressure.

For structural support and alinement purposes a solid cylindrical housing was used to connect the front and rear bearing housings (fig. 2). The diffuser downstream of the last stator directed the argon gas radially outward into the single outlet collector which had a constant circular cross section. Figure 3 shows the assembled compressor package (uninsulated) as installed in the test facility. In order to minimize heat transfer during compressor testing, the compressor assembly was insulated with a high temperature granular insulating material which was contained by a box built around the compressor package. Insulating material was also placed between the compressor support structure and test stand bedplate. A photograph of the compressor fully insulated is shown in figure 4.

Test Facility

With the exception of the compressor package and compressor piping modification, the test facility used in this investigation is the same as described in reference 5. Figure 5 is a schematic flow diagram of the test facility.

Instrumentation

Flow through the compressor was determined from pressure and temperature measurements at a thin-plate orifice installed according to ASME standards in the compressor gas supply line (fig. 5). Compressor performance was based on pressure and temperature measurements at three instrument stations: (1) inlet station located about 10 inches (25.4 cm) upstream of inlet flange, (2) stator 6 exit station, and (3) collector exit station located about 3 inches (7.6 cm) downstream of exit flange. Combination total pressure-temperature rakes were employed at the inlet and exit pipe stations. The cross-sectional area at both inlet and collector exit station was divided into three equal annular areas. Total pressure sensing heads were placed at the arithmetical center of each area. Copper-constantan spike-type thermocouples were placed between the total pressure heads. Three combination total pressure-temperature rakes were placed 120° apart at the inlet pipe station and four combination rakes (equally spaced) were used at the collector exit station. A photograph of a sample rake is presented in figure 6. Wall static pressure taps of 0.030-inch (0.076-cm) diameter were installed at the inlet and exit pipe stations circumferentially midway between rakes.

Instrumentation at the exit of stator 6 consisted of two sets of five individual total pressure probes, two sets of five individual total temperature probes, four outer wall static pressure taps, and four inner wall static pressure taps. A photograph of the probes installed at stator 6 exit is shown in figure 7. The two sets of total pressure probes were placed circumferentially 180° apart as were the two sets of temperature probes. The static pressure taps were placed circumferentially 90° apart. The total pressure probes were of the shielded type. The heads of the individual probes of one set were located circumferentially to be alined with a stator midspacing and radially (starting from the outer wall) at 10, 30, 50, 70, and 90 percent of the stator passage height. The heads of the probes of the other set were all located radially at 50 percent of passage height and circumferentially to span the equivalent of a stator spacing. The spacing of the second set of probes was positioned to provide some indication of the total pressure defect due to the wake of the sixth stator at the midpassage location. This information was then used to adjust the free stream (midspacing) measurements obtained from the other set of probes. The method of making this adjustment is discussed in the section Calculation Procedure.

The total temperature probes at the exit of stator 6 were of a semishielded type employing copper-constantan wire. The thermocouple junction of the two sets of five individual probes were located circumferentially at stator midspacings and radially at 10, 30, 50, 70, and 90 percent of passage height, the same as the one set of total pressure probes.

In addition to the instrumentation at the three locations described, static pressure wall taps were installed throughout the compressor. Compressor speed was sensed by a magnetic pickup in conjunction with a gear mounted on the compressor shaft.

Strain-gage-type transducers were employed to measure all pressures. A constant reference temperature oven (150° F or 66° C) was used with the research thermocouples in obtaining temperature measurements. An automatic digital potentiometer was used to record the measurements on paper tape for computor processing of the data. Estimated accuracy of measurement is as follows: pressure, ±1.5 percent; temperature, $\pm 1.5^{\circ}$ R (±0.8 K); and speed, ±0.5 percent.

Test Procedure

Compressor test data were taken over a range of weight flows from maximum flow to stall conditions at 50, 60, 70, 80, 90, and 100 percent equivalent design speed. All data were taken at a nominal design inlet pressure and temperature of 6 psia (41×10^3 N/m^2 abs) and 536° R (298 K), respectively.

During the test program, it was found that thermal equilibrium in the compressor took much longer to establish than expected. This may in part be attributed to the low flow rate as compared to the mass of metal involved in the housing structural members of the test package. Figure 8 shows the measured temperature rise across the compressor ratioed to inlet temperature as a function of time for various wheel speeds. These curves were obtained by first establishing thermal equilibrium near maximum flow for a given speed and then rapidly changing the flow rate to that near maximum efficiency. After the change in flow (at time zero in the figure), data points were recorded every few minutes. At 60 percent of design speed it took more than 20 minutes to approach equilibrium. At the higher speeds and therefore higher flow rates this time was slightly reduced. These changes in measured temperature rise can result in changes in apparent efficiency as large as 4 to 6 percentage points. To accurately establish the compressor efficiency using the measured temperature rise of the gas, it is essential that thermal equilibrium be established. Therefore, the data points presented herein were taken at time intervals greater than 20 minutes.

Calculation Procedure

Compressor performance was calculated from pressure and temperature measurements taken at the orifice located in the inlet argon supply line, the compressor inlet station, the stator 6 exit station (station 7), and the collector exit station (station 8). Although the total temperature measurements at the exit of the sixth stator and at the collector exit should theoretically agree, it was found that temperatures at stator 6 exit were consistently higher (about 14° to 26° R or 8 to 14 K at design speed). It is felt that this discrepancy is caused by a heat loss from the system and thermal conduction errors in the exit plane temperature rakes. In spite of the effort to fully insulate the compressor package, there are at least three paths for heat transfer from the compressor gas between stations 7 and 8:

(1) Heat transfer to the lubricating oil

(2) Heat transferred along the exit pipe to the uninsulated end

(3) Heat loss from an uninsulated section of the diffuser and collector (near the drive coupling) to the drive turbine exhaust air

The effect of the heat loss to the lubricating oil was evaluated by the same method used in reference 9. At design speed and flow the lubricating oil lowers the compressor exit temperature by $2\frac{1}{2}^{\circ}$ R (1.4 K).

The outer ring of thermocouples in the collector exit station indicate a temperature 2.5° R (1.4 K) lower than the inner ring at design speed and flow. It is reasoned that the outer thermocouples may be effected by thermal conduction down the stems of the rakes. In examining the data it was noted that the wall to which the rakes are attached is 34° R (19 K) below stream temperature and this could contribute to this error. This cooler wall is also an indication of the size of the heat loss from the exit flow.

For reasons apparent in the previous discussion, the collector exit station temperatures were not used. The temperature measured at the sixth stator exit was assumed correct in establishing the temperature rise across the compressor and was used in calculating compressor efficiency.

The size and compactness of the compressor limited the amount of instrumentation which could be installed at stator 6 exit. For this reason instrumentation to measure the total pressure defect due to the wake of the sixth stator was installed at 50 percent of passage height only. This pressure defect at 50 percent of passage height was then used to adjust the free stream (midspacing) total pressure measurements obtained at 10, 30, 70, and 90 percent of passage height to approximate the average total pressure at these locations. The free stream total pressure at these locations was reduced by the ratio of the average total pressure obtained from the five probes positioned at 50 percent passage height and spanning the equivalent of a stator spacing to the free stream total pressure measured at that location. This technique will tend to account for the defect in total

pressure resulting in the stator wake at the other locations. If the defect in total pressure resulting from the last stator in actuality were constant across the span, no error in stator exit total pressure would be introduced in obtaining the average pressure across the passage in this manner. However, it is likely that the total pressure defect will increase in the end wall regions as a result of larger stator wakes in these regions as the reflection of higher total pressure losses. No attempt was made to account for the potentially higher losses in the end wall regions in reducing the data. Therefore, the data presented herein on the performance of the compressor based on measurements taken at the compressor inlet and stator 6 exit may be slightly higher than the true performance. In terms of efficiency it is estimated that this error would result in the indicated efficiency being no more than one percentage point higher than the true efficiency.

Mass averaged values of pressures and temperatures were used in computing total pressure ratio and efficiency. In computing these mass averaged values at stator 6 exit station, a linear static pressure was assumed between tip and hub wall static pressures. Equations used in computing compressor performance are defined in the section SYMBOLS.

RESULTS AND DISCUSSION

The data presented herein were obtained from a 3.7-inch (9.4-cm) diameter six-stage axial-flow compressor operated in argon.

Overall Performance

Compressor inlet to collector exit. - Overall performance from station 0 to station 8 is presented in figure 9. (The tailed data points presented in fig. 9 are those for which the wall static pressure rise through the compressor are presented in fig. 11 and discussed later.) Total pressure ratio and adiabatic efficiency as a function of equivalent argon weight flow are presented for six speeds. Peak efficiency at the design equivalent rotative speed of 49 213 rpm was 0.755 and occurred at an equivalent weight flow of 1.55 pounds per second (0.70 kg/sec). The pressure ratio at peak efficiency was 2.72. The design values of efficiency, weight flow, and pressure ratio were 0.825, 1.52 pounds per second (0.69 kg/sec), and 2.3, respectively.

Peak efficiency values for each of the six speeds as indicated in figure 9 increased as speed decreased from 0.756 at design speed to 0.77 at 80 percent design speed. Below 80 percent of design speed, the peak efficiency decreased to a low of 0.735 at 50 percent speed.

The peak efficiency at design speed is lower than the design value; however, as noted, the total pressure ratio is considerably above design. Since there was no interstage instrumentation other than wall static pressures, a detailed explanation for the increase above the expected total pressure rise cannot be given. It is assumed however that the actual deviation angles are less than design which results in an increase in work input (temperature ratio) and work output (pressure ratio). As noted in the design section, design deviation angles were increased above values arrived at by normal design rules based on data presented in reference 8. The data presented in this reference indicated that an increase in deviation angle could be expected at the low Reynolds number at which the blading must operate for this compressor. It is probable that, at least for this compressor, an increase in deviation angle resulting from the low Reynolds numbers did not materialize.

An increase in pressure above the design value (which may be attributed to lower than design deviation angles as reasoned previously) results in a decrease in axial velocity which further increases turning and thus work. It is also possible that the allowance for boundary layer growth through the machine was larger than actual boundary layer growth resulting in a larger effective flow area than assumed in the design. This would also result in a decrease in axial velocity and an increase in work.

The higher than design pressure should cause some mismatching of flow angles in the compressor. A further mismatching could occur from lower than design deviation angles. This mismatching could explain the lower than design efficiency obtained.

The slight increase in peak efficiency as speed is decreased to 80 percent speed may in part be a result of the compressor operating closer to the design overall density ratio at part speed than at design speed because of the higher than design pressure ratio at design speed. Therefore, the blading of the front and rear stages may be operating closer to these design incidence angles at part speed than at design speed.

Compressor inlet to stator 6 exit. - Performance of the compressor from station 0 to station 7 is presented in figure 10. Peak efficiency at design speed was 0.78 and occurred at a weight flow of 1.56 pounds per second (0.71 kg/sec). The pressure ratio at peak efficiency was 2.76. The design values of efficiency, weight flow, and pressure ratio were 0.825, 1.52 pounds per second (0.69 kg/sec), and 2.30, respectively. At peak efficiency the loss in the diffuser and collector account for 2.4 percentage points in efficiency. Peak efficiency values for each of the six speeds follow the same trend as the overall performance (stations 0 to 8) with the highest values occurring near 80 percent speed.

Static Pressure Rise Through Compressor

Wall static pressure distribution through the compressor operating at design speed

is presented in figure 11 for the tailed data points presented in figure 9. The design static pressure distribution is also shown in figure 11. The static pressure at the inlet of rotor 2 and stator 4 is missing due to transducer failure. It is apparent that for the compressor operating at or near design weight flow there is a consistent higher than design static pressure rise throughout the compressor. This higher than design static pressure gradient through the machine indicates the increase in work through the machine above design values was uniform. As indicated earlier, this may be a result of the deviation angles being less than design and/or the boundary layer blockage being less than design.

CONCLUDING REMARKS

A 3.7-inch (9.4-cm) diameter six-stage axial-flow compressor suitable for a 10-kilowatt solar Brayton cycle power generation system was tested in argon. The overall performance for the compressor is presented based on compressor inlet - collector exit gas conditions and compressor inlet - stator 6 exit conditions.

Peak efficiency (compressor inlet to collector exit) was 0.755 at the design equivalent rotative speed of 49 213 rpm and occurred at an equivalent weight flow of 1.55 pounds per second (0.70 kg/sec). The pressure ratio at peak efficiency was 2.72. The design values of efficiency, weight flow, and pressure ratio were 0.825, 1.52 pounds per second (0.69 kg/sec), and 2.30, respectively.

Excluding the total pressure losses which occurred in the diffuser and collector (compressor inlet to stator 6 exit performance), the compressor achieved a peak efficiency of 0.78 and a corresponding pressure ratio of 2.76 at design speed. The design values of efficiency and pressure ratio excluding the estimated losses in the diffuser and collector were 0.858 and 2.365, respectively.

A possible explanation of the increased total pressure rise above design values may be due in part to actual deviation angles being lower than those assumed in the design. This may have resulted from overcompensating for Reynolds number effect on deviation angle in arriving at design values. A further possibility is that the actual effective flow area is greater than that assumed in the design. The lower than design efficiency may in part be a result of the mismatching of flow angles within the machine due to the higher than design pressure ratio.

Lewis Research Center,
National Aeronautics and Space Administration,
Cleveland, Ohio, November 9, 1970,
120-27.

REFERENCES

1. Stewart, Warner L.; Glassman, Arthur J.; and Krebs, Richard P.: The Brayton Cycle for Space Power. Paper 741 A, SAE, Sept. 1963.

2. Bernatowicz, Daniel T.: NASA Solar Brayton Cycle Studies. Presented at the Symposium on Solar Dynamic Systems, Solar and Mechanical Working Groups of the Interagency Advanced Power Group, Washington, D.C., Sept. 1963.

3. Glassman, Arthur J.: Summary of Brayton Cycle Analytical Studies for Space-Power System Applications. NASA TN D-2487, 1964.

4. Kofsky, Milton G.; and Glassman, Arthur J.: Turbomachinery Characteristics of Brayton-Cycle Space-Power-Generation Systems. Paper 64-GTP-23, ASME, Mar. 1964.

5. Tysl, Edward R.; Ball, Calvin L.; Weigel, Carl; and Heidelberg, Lawrence J.: Overall Performance in Argon of a 6-Inch Radial-Bladed Centrifugal Compressor. NASA TM X-1622, 1968.

6. Anon.: Design and Fabrication of a High-Performance Brayton-Cycle Compressor Research Package. Rep. APS-5109-R, AiResearch Mfg. Co. (NASA CR-54368), May 1965.

7. Cohen, R.; Gilroy, W. K.; and Marchant, R. D.: Compressor Research Package for Research and Development of High Performance Axial-Flow Turbomachinery. Rep. PWA-2933, Pratt & Whitney Aircraft (NASA CR-54884), Mar. 1967.

8. Rhoden, H. G.: Effect of Reynolds Number on the Flow of Air Through a Cascade of Compressor Blades. Rep. R&M 2919, Ministry of Supply, Aeronautical Research Council, 1956.

9. Heidelberg, Laurence J.; Ball, Calvin L.; and Weigel, Carl: Effect of Reynolds Number on Overall Performance of a 6-Inch Radial Bladed Centrifugal Compressor. NASA TN D-5761, 1970.

TABLE I. - VALUES OF COMPRESSOR DESIGN PARAMETERS

[Working fluid: argon.]

Compressor design parameters	Based on design inlet pressure and temperature	Based on standard inlet pressure and temperature
Compressor inlet total pressure, P_0, psia (N/m^2 abs)	6 (41×10^3)	14.7 (101×10^3)
Compressor inlet total temperature, T_0, ^oR (K)	536 (298)	518.7 (288.2)
Weight (mass) flow rate, W, lb/sec (kg/sec)	0.611 (0.278)	1.52 (0.69)
Compressor total pressure ratio, P_7/P_0	2.365	[a]2.365
Compressor total pressure ratio, P_8/P_0	2.3	[a]2.3
Compressor adiabatic efficiency, η_{0-7}	0.858	[a]0.858
Compressor adiabatic efficiency, η_{0-8}	0.825	[a]0.825
Compressor total temperature ratio, $T_7/T_0 = T_8/T_0$	1.494	[a]1.494
Compressor rotational speed, N, rpm	50 000	49 183

[a]Approximate equivalent values which may differ from design values as a result of differences in Reynolds numbers between design and standard inlet conditions.

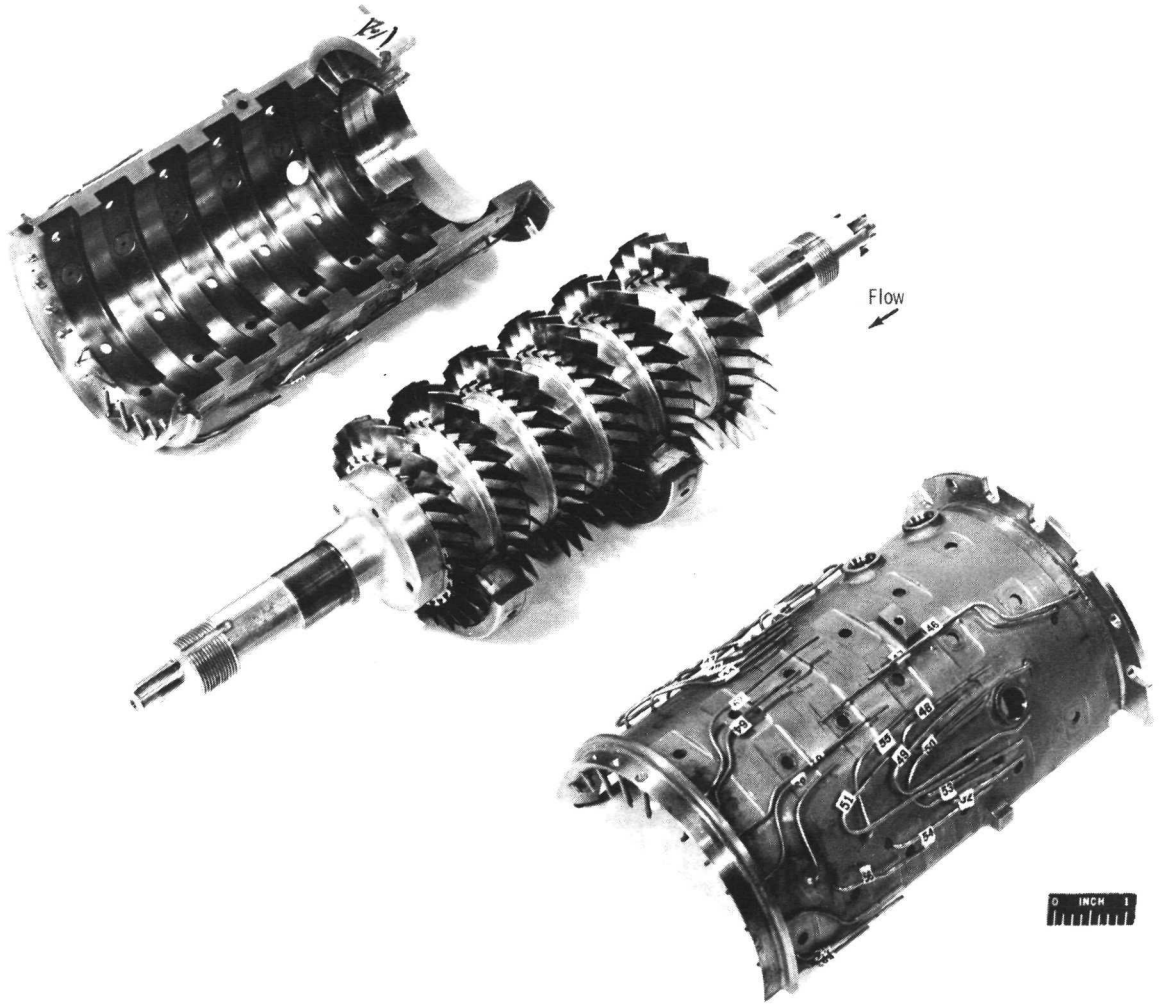

C-66-4625

Figure 1. - Six-stage rotor and split casing.

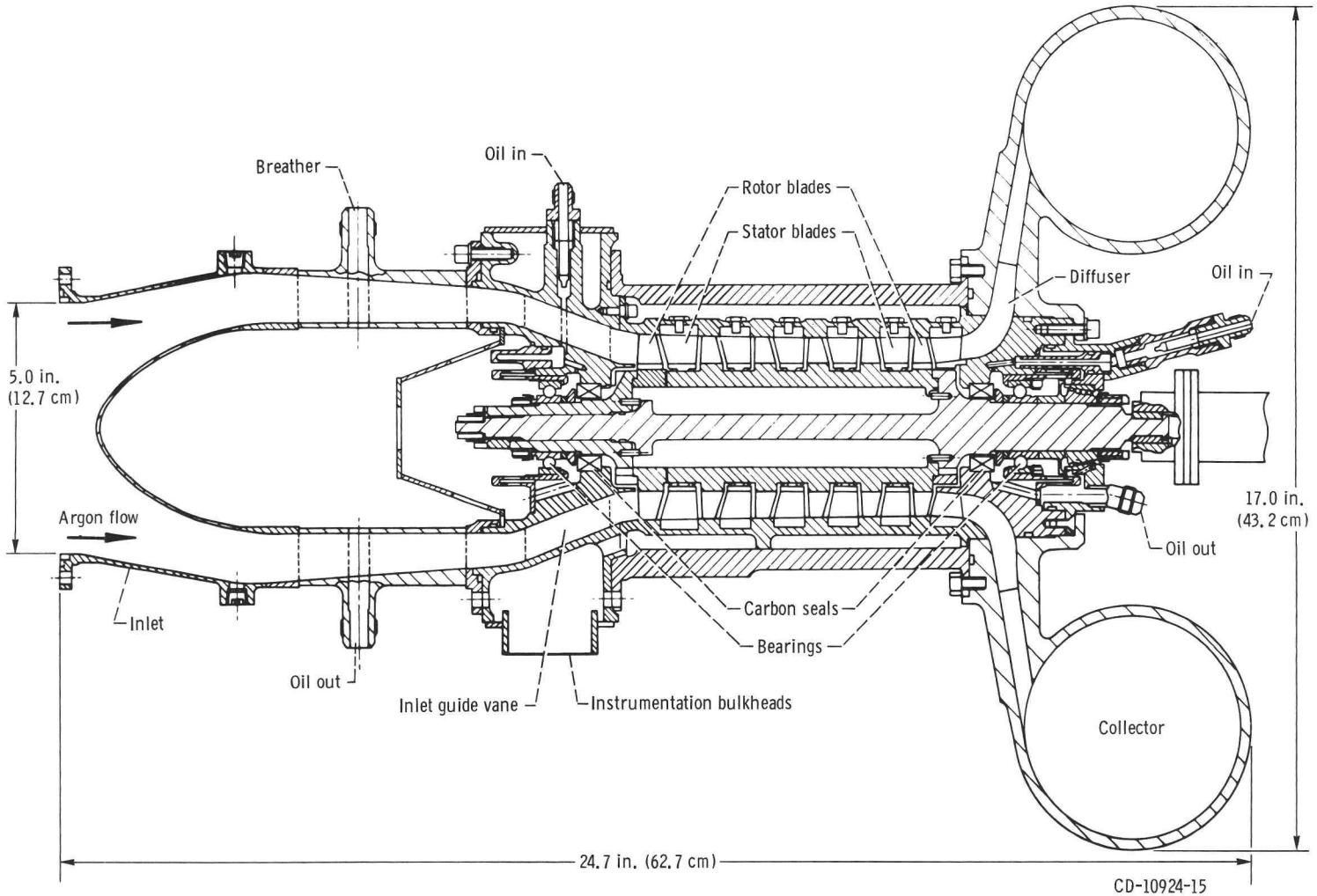

Figure 2. - Cross section of compressor research package.

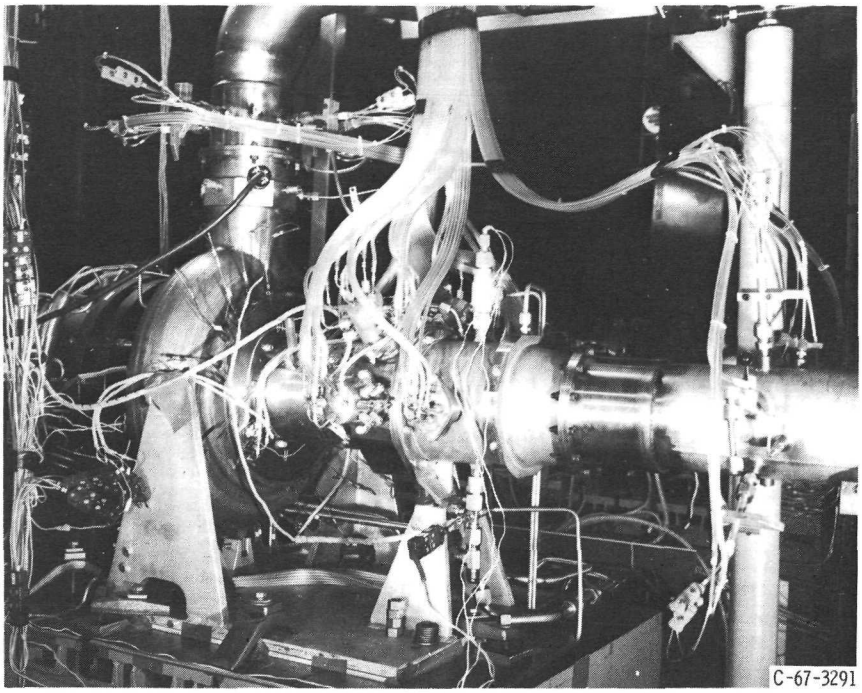

Figure 3. - Compressor package.

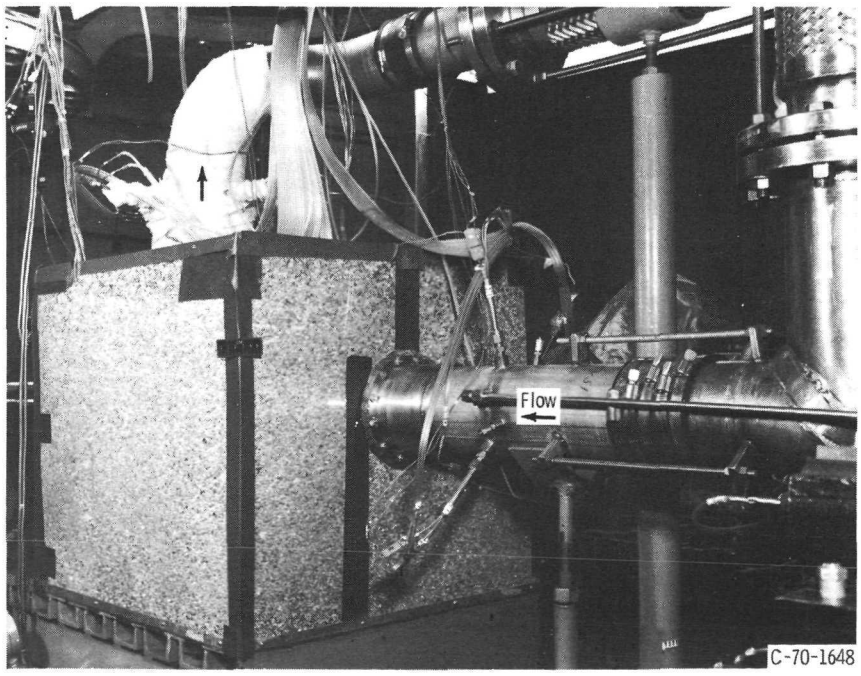

Figure 4. - Compressor fully enclosed in insulation.

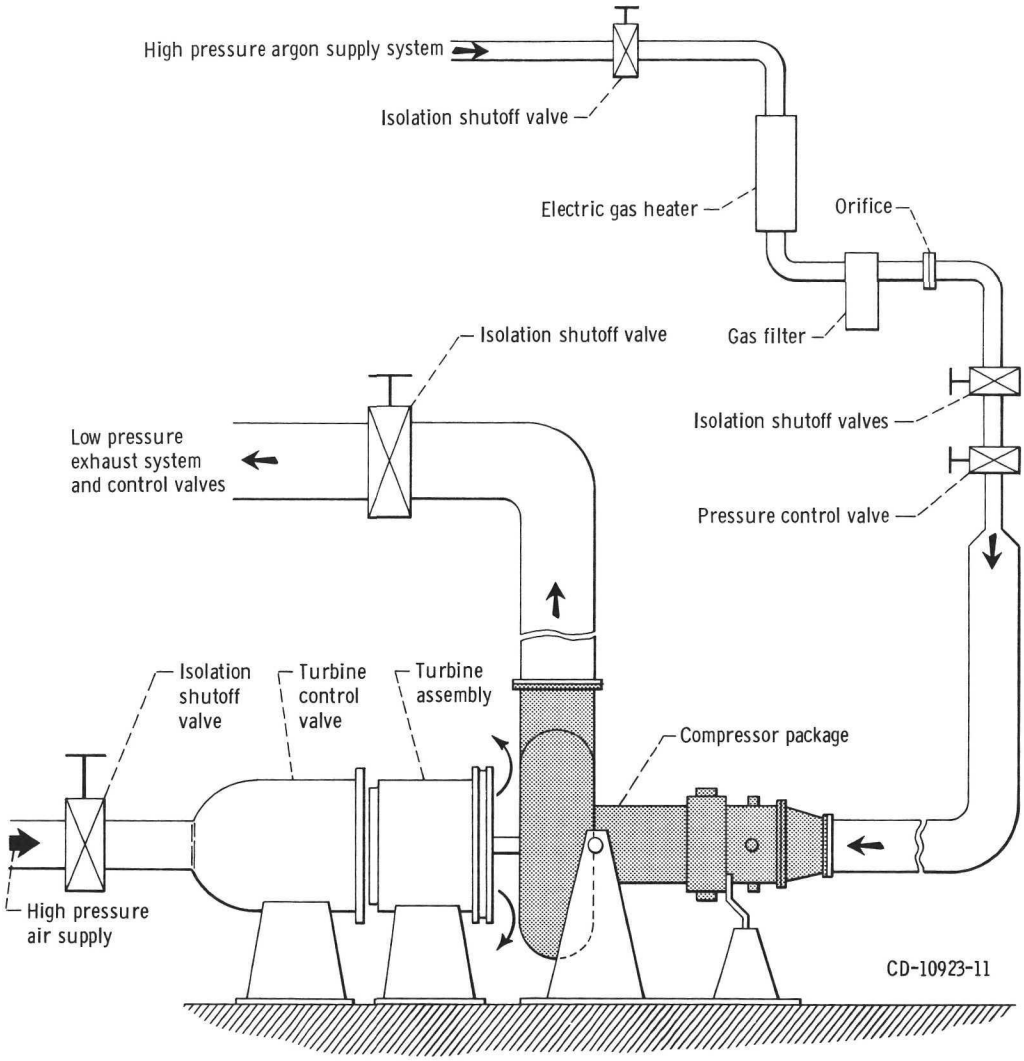

Figure 5. - Flow diagram of compressor test facility.

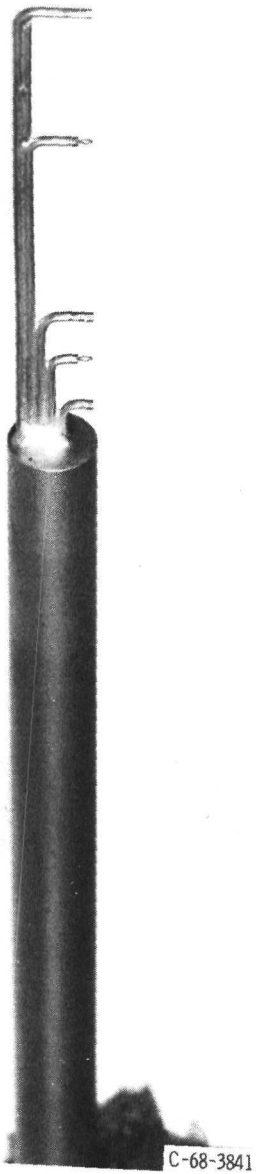

Figure 6. - Combination total pressure and total temperature rake.

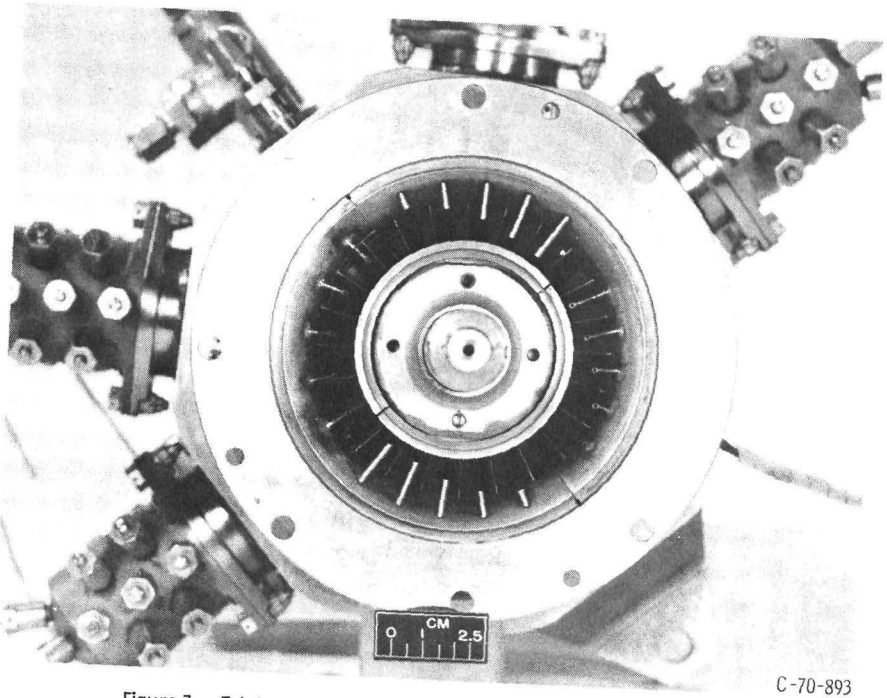

Figure 7. - Total pressure and total temperature probes at stator 6 exit.

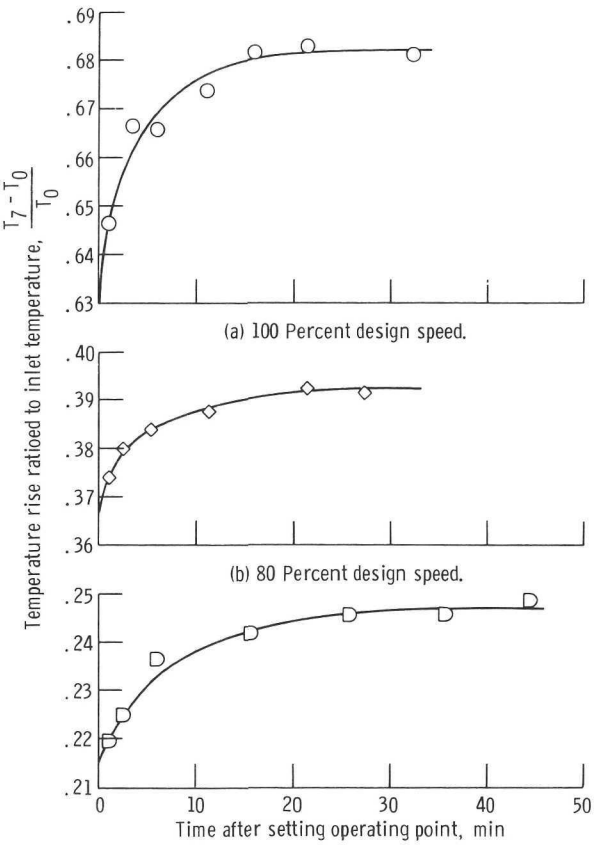

(a) 100 Percent design speed.

(b) 80 Percent design speed.

(c) 60 Percent design speed.

Figure 8. - Effect of time on temperature rise ratioed to inlet temperature.

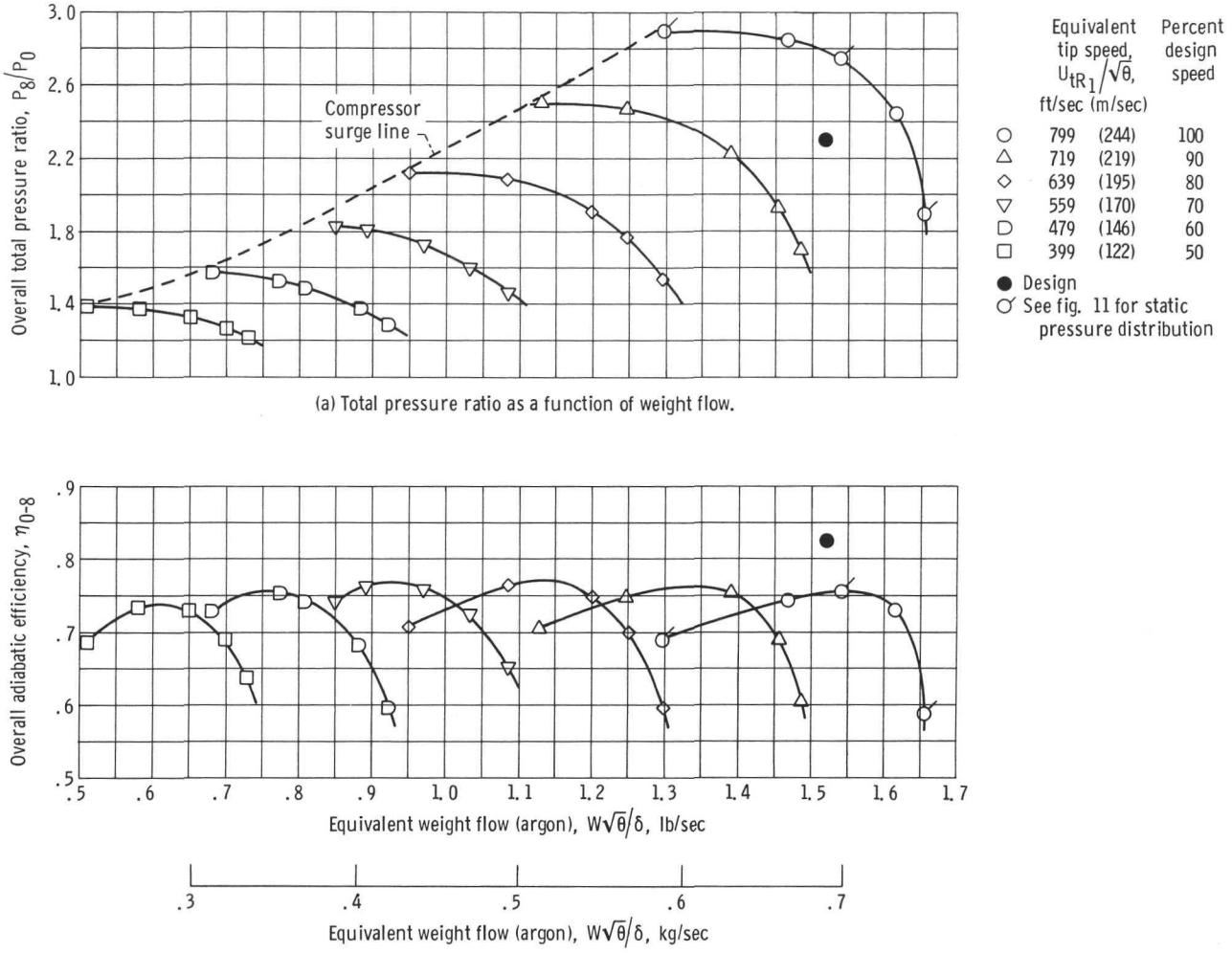

(a) Total pressure ratio as a function of weight flow.

(b) Overall efficiency as a function of weight flow.

Figure 9. - Overall performance of 3.7-inch (9.4-cm) six-stage axial-flow compressor. (Inlet flange to collector exit, station 0 to 8.)

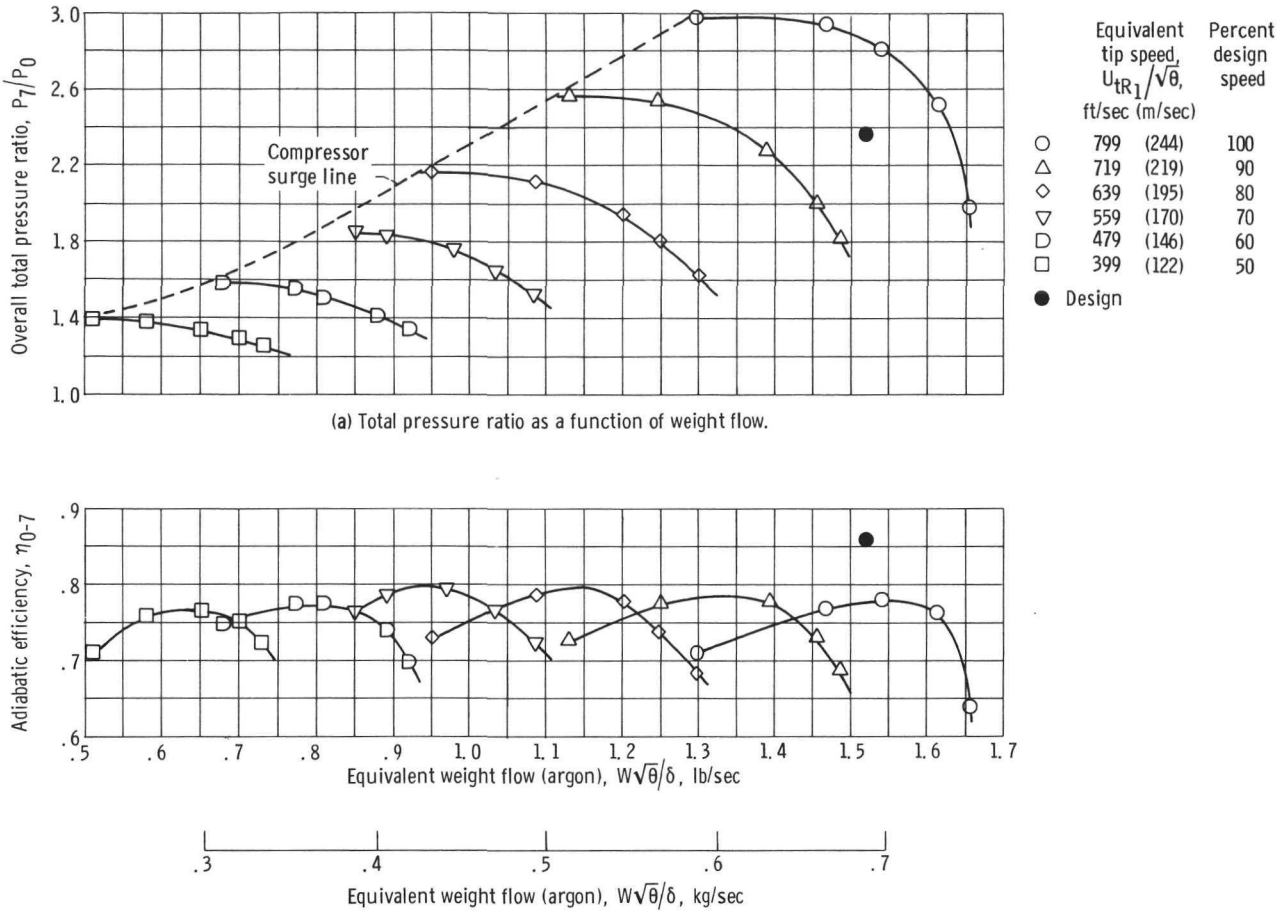

(a) Total pressure ratio as a function of weight flow.

(b) Efficiency as a function of weight flow.

Figure 10. - Overall performance of 3.7-inch (9.4-cm) six-stage axial-flow compressor. (Inlet flange to stator 6 exit, station 0 to 7.)

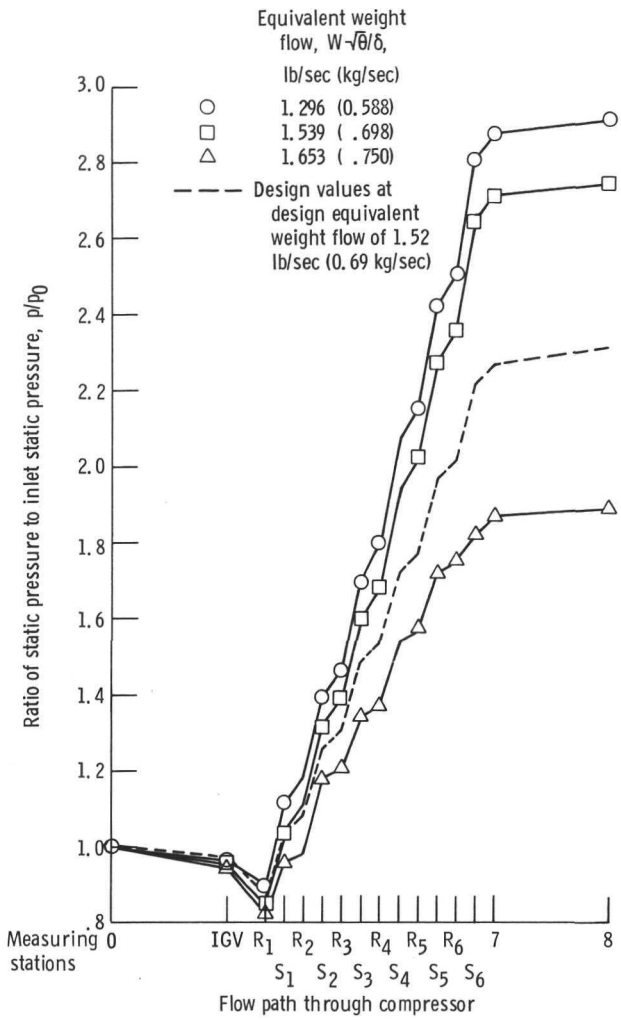

Figure 11. - Comparison of experimental and calculated static pressure distribution at design speed.

NATIONAL AERONAUTICS AND SPACE ADMINISTRATION
WASHINGTON, D.C. 20546

OFFICIAL BUSINESS

FIRST CLASS MAIL

POSTAGE AND FEES PAID
NATIONAL AERONAUTICS AND
SPACE ADMINISTRATION

POSTMASTER: If Undeliverable (Section 158 Postal Manual) Do Not Return

"The aeronautical and space activities of the United States shall be conducted so as to contribute . . . to the expansion of human knowledge of phenomena in the atmosphere and space. The Administration shall provide for the widest practicable and appropriate dissemination of information concerning its activities and the results thereof."

—NATIONAL AERONAUTICS AND SPACE ACT OF 1958

NASA SCIENTIFIC AND TECHNICAL PUBLICATIONS

TECHNICAL REPORTS: Scientific and technical information considered important, complete, and a lasting contribution to existing knowledge.

TECHNICAL NOTES: Information less broad in scope but nevertheless of importance as a contribution to existing knowledge.

TECHNICAL MEMORANDUMS: Information receiving limited distribution because of preliminary data, security classification, or other reasons.

CONTRACTOR REPORTS: Scientific and technical information generated under a NASA contract or grant and considered an important contribution to existing knowledge.

TECHNICAL TRANSLATIONS: Information published in a foreign language considered to merit NASA distribution in English.

SPECIAL PUBLICATIONS: Information derived from or of value to NASA activities. Publications include conference proceedings, monographs, data compilations, handbooks, sourcebooks, and special bibliographies.

TECHNOLOGY UTILIZATION PUBLICATIONS: Information on technology used by NASA that may be of particular interest in commercial and other non-aerospace applications. Publications include Tech Briefs, Technology Utilization Reports and Technology Surveys.

Details on the availability of these publications may be obtained from:

SCIENTIFIC AND TECHNICAL INFORMATION OFFICE

NATIONAL AERONAUTICS AND SPACE ADMINISTRATION

Washington, D.C. 20546